

# Computational investigation on interaction between graphene nanostructure BC<sub>3</sub> and Rimantadine drug: Possible sensing study of BC<sub>3</sub> and its doped derivatives on Rimantadine

Ayda karbakhshzadeh <sup>a,\*</sup>, Soma Majedi <sup>b</sup>, Vahideh Abbasi <sup>c</sup>

<sup>a</sup> Department of Chemistry, Faculty of Science, Azarbaijan Shahid Madani University, Tabriz, Iran

<sup>b</sup> Medical Analysis Department, Faculty of Science, Tishk International University, Erbil, Kurdistan Region, Iraq.

<sup>c</sup> Department of Chemistry, University of Zanjan, Zanjan, Iran

## ARTICLE INFO

### Article history:

Received 30 May 2022

Received in revised form 10 June 2022

Accepted 15 July 2022

Available online 24 July 2022

### Keywords:

Rimantadine

Diamondoid

Sensor

Graphene-like BC<sub>3</sub>

Density functional theory (DFT)

## ABSTRACT

The purpose of this computational study is to measure and evaluate the interaction between rimantadine drug with different plate-like nanostructures.

The interactions between the diamondoid rimantadine molecule and nanosheets including graphene, boron-doped graphene (BC<sub>3</sub>), and aluminum, silicon, phosphorus and gallium doped BC<sub>3</sub> have been studied using the B3LYP method with a basis set of 6-31G(d) by Gaussian software 09. A poor energy interaction between the rimantadine drug molecule and the graphene nanoparticle was observed. The E<sub>ad</sub> (adsorption energy) and E<sub>g</sub> (gap energy) of BC<sub>3</sub> and Al-, Si-, P-, Ga-doped BC<sub>3</sub> nanosheets with rimantadine have been calculated. The results show that the Si-doped BC<sub>3</sub> nanoparticle is the best sensor for rimantadine drug.

## 1. Introduction

Diamondoids (also called nanodiamonds) are cage saturated hydrocarbon molecules that can be superimposed on the diamond lattice.<sup>1</sup> Thus diamondoids which resemble parts of the diamond lattice, are members of the carbon nanostructure family. The simplest of these diamondoids, with the common name “adamantane”, is a tricyclic C<sub>10</sub>H<sub>16</sub> isomer. Diamondoids are very attractive nanoscale building blocks (0.5–2 nm).<sup>2</sup> The most widely known functionalized adamantane is 1-aminoadamantane (also known as amantadine), which is both an antiviral and anti-parkinson drug.<sup>3</sup> Graphene is a term used to describe very thin strips of graphite monolayers. If we consider graphite as a booklet of parallel sheets, each sheet is called graphene. Graphene is called the magic of the 21st century.<sup>4,5</sup> This material, which is the strongest material studied to date, is said to be a good alternative to silicon. The strange and magical properties of graphene, such as: high electrical conductivity, hardness, very high mechanical strength, excellent optical and surface

properties, and high and adjustable thermal conductivity, have made the world of science and media think and research about this material. Graphene is known as an electrical conductor in the absence of a band gap. In a graphene sheet, each carbon atom has a free bond outside the sheet.<sup>6</sup> This bond is a good site to put some functional groups as well as hydrogen atoms. The bond between the carbon atoms here is covalent and very strong.<sup>7,8</sup> The BC<sub>3</sub> nanoplate has a geometric structure almost identical to that of graphene nanoplates, except that some of the carbon atoms in the graphene nanoplate have been replaced by boron atoms (so that the carbon atoms are surrounded by boron atoms) to form a nanosheet called BC<sub>3</sub>.<sup>9</sup> It should be noted that the BC<sub>3</sub> nanosheet is an indirect semiconductor with a gap, while the graphene nanosheet is a zero semiconductor. Theoretical research has shown that the electronic properties of the BC<sub>3</sub>

nanosheet are amazingly adjustable.<sup>10</sup> At 300 to 600 K the BC<sub>3</sub> monolayer nanosheet can maintain its structure well, even at temperatures above 1000 K it can withstand minor deviations that are not sufficient to destroy the C-

\* Corresponding author. e-mail: [Ida.karbakhsh@gmail.com](mailto:Ida.karbakhsh@gmail.com)

C and C-B bonds. If one of the carbons in the BC3 structure is replaced by nitrogen, the structure is displayed as BC2N. By doping aluminum, silicon, phosphorus, gallium, etc. atoms into BC3 nanostructure, doped BC3 nanosheets can be formed with each of the atoms.<sup>11,12</sup>

## 2. Computer details

Density citizenship theory is used as a useful computational method for calculating electronic correlations and can often produce MP2 computational quality results almost simultaneously with the time required for computations (HF).<sup>13</sup> The energy of the n-electron system can be expressed in terms of the electron probability density. That is, the density as a whole is a function of spatial coordinates, which is called the DFT method.<sup>14,15</sup> In the DFT method, the electronic energy of the system, based on the Cohen-Sham equation, is written as follows.

$$\varepsilon = \varepsilon_T + \varepsilon_V + \varepsilon_J + \varepsilon_{XC} \quad (1)$$

Where  $\varepsilon_T$  is the expression for kinetic energy that increases with the motion of electrons. And  $\varepsilon_V$  The term energy is a potential that includes nucleus-electron and nucleus-nucleus interactions.  $\varepsilon_J$  The term energy is an electron repulsion - electron.  $\varepsilon_{XC}$  It is related to the correlation energy and the exchange of electrons.<sup>16</sup>

Different DFT methods are obtained by combining different types of exchange functions with correlation functions. In this research, GaussView graphic software is used to draw complexes. In order to optimize the desired complexes, Gaussian09 software has been used in Linux operating system.

Among the DFT methods, the B3LYP method is widely used in chemical processes and is used for large molecules and complex systems. In the B3LYP method, the Beck gradient correction exchange function is combined with the Li, Yang, and Par gradient correlation function. In general, in the B3LYP method, the number 3 indicates the application of three experimental parameters in the Beck exchange function.<sup>18</sup>

## 3. Results and Discussion

The absorption of amantadine on nanoparticles is very important. The purpose of this research is the ability of graphene nanoparticles to absorb and detect amantadine and whether it is a sensor. It is important in the ability of the sensor to be the two factors of energy absorption and the Lumo-Homo difference. The adsorption energy must

be within the normal range and suitable range for both adsorption and desorption. In this case, it can be said that the nanoparticle can act as a sensor. In addition, if the drug is adsorbed on nanoparticles, the Homo-Lumo difference must be reduced to increase the electrical conductivity of graphene nanoparticles due to the adsorption of Rimantadine on its outer wall, which forms the basis of BC3 graphene sensors. Our main goal is to use the density density theory (DFT) calculations to theoretically investigate the electrical sensitivity of graphene, BC3 nanostructures and their doped forms, as well as to investigate whether or not the adsorption and desorption of Rimantadine molecule on graphene and BC3 nanosheets are favorable. And its duplicated forms. According to the formula of absorption energy:

$$E_{ad} = E_{\text{adsorption}} = E_{\text{Complex}} - E_{\text{nano}} - E_{\text{drug}} + \text{BSSE} \quad (2)$$

Where  $E_{(\text{nano})}$  the total energy of the nanosheet,  $E_{(\text{drug})}$  Total energy of the drug Rimantadine,  $E_{(\text{Rimantadine / adsorbent})}$  The total energy of the drug amantadine absorbed on the adsorbent surface and  $E_{(\text{BSSE})}$  The matching error is the base set for all absorption energies. The closer the amount of adsorption energy or ( $E_{\text{adsorption}}$ ) is to the range of 20, the more stable the complex will be. But this theory also depends on another factor called energy gap.<sup>19</sup> To get %  $\Delta E_g$  you have to use the following equation:

$$E_{\text{gap}} = E_g = E_{\text{LUMO}} - E_{\text{HOMO}} \quad (3)$$

$$\% \Delta E_g = (E_{g-\text{complex}} - E_{g-\text{nano}}) / E_{g-\text{nano}} \times 100 \quad (4)$$

The larger the %  $\Delta E_g$  complex, the greater the nanosheet sensitivity to the drug. As a result, the nanosheet is a good sensor for the drug.

In this research, two tables have been considered for possible complexes between amantadine drug molecule and graphene nanosheets, BC3 and BC3 nanosheets doped with Si, Al, P, Ga atoms. In the first table (Table1), the absorption energy and bond length are changed, and in the next table (Table2), the Homo and Lomo energies are examined in terms of electron volts and Hartree, as well as their stiffness. The difference in energy levels between Homo and Lumo indicates electrical conductivity. Also to compare whether amantadine interacts better with graphene sensors or with BC3 nanosheet and its doped forms, One of the boron atoms of nanosheet BC3 has been replaced with atoms of silicon, phosphorus, gallium and aluminum and the resulting absolute energy, bond length, Homo energy, and Lumo complexes have been investigated.

**Table 1.** Comparison of energy of raw materials, products and enthalpy changes

Nano structure	$E_{\text{HOMO}}$ ( au )	$\Delta E_t = E_{\text{HOMO}} - E_{\text{LUMO}}$ ( au )	( kcal/mol ) $\Delta E_t$
Rimantadine-BC <sub>3</sub>	-4107/56	-0/038	-23/96
Rimantadine-BC <sub>3</sub> -Al	-4325/07	-0/045	-28/72
Rimantadine-BC <sub>3</sub> -Si	-4372/06	-0/030	-19/32
Rimantadine-BC <sub>3</sub> -Ga	-6005/46	-0/032	-20/41
Rimantadine-BC <sub>3</sub> -P	-4424/02	-0/032	-20/31
Rimantadine-Graphene	-4425/59	-0/0032	-2/068

**Table 2.** Comparison of Homo, Lomo and Hardness Energy for Thirteen Possibilities of Rimantadine Approaching Graphene, BC<sub>3</sub> Nanosheets and Doped Derivatives

Nano structure	$E_{\text{HOMO}}$ (H)	$E_{\text{HOMO}}$ (eV)	$E_{\text{LUMO}}$ (H)	$E_{\text{LUMO}}$ (eV)	$\eta(\text{H}) = \epsilon_L - \epsilon_H$	$\eta(\text{eV}) = \epsilon_L - \epsilon_H$	$\Delta E_g$ %
BC <sub>3</sub>	-0/23	-6/46	-0/137	-3/74	0/099	2/71	-
BC <sub>3</sub> -AL	-0/22	-6/18	-0/136	-3/71	0/090	2/47	-
BC <sub>3</sub> -Si	-0/18	-5/04	-0/137	-3/74	0/047	1/30	-
BC <sub>3</sub> -Ga	-0/22	-6/16	-0/136	-3/71	0/088	2/41	-
BC <sub>3</sub> -P	-0/21	-5/93	-0/137	-3/75	0/079	2/17	-
Graphene	-0/13	-3/77	-0/131	-3/59	0/006	0/18	-
Rimantadine	-0/20	-5/67	-0/069	-1/88	0/139	3/79	-
Rimantadine-BC <sub>3</sub>	-0/22	-6/18	-0/134	-3/66	0/092	2/51	-7/4
Rimantadine-BC <sub>3</sub> -Al	-0/20	-5/66	-0/130	-3/55	0/077	2/11	-14/3
Rimantadine-BC <sub>3</sub> -Si	-0/15	-4/09	-0/129	-3/52	0/02	0/56	-56/6
Rimantadine-BC <sub>3</sub> -Ga	-0/21	-5/85	-0/134	-3/66	0/08	2/19	-9/14
Rimantadine-BC <sub>3</sub> -P	-0/21	-5/83	-0/130	-3/55	0/083	2/28	4/9
Rimantadine-Graphene	-0/13	-3/74	-0/130	-3/56	0/006	0/18	0

## 4. Experimental

### 4.1. Rimantadine drug complexes and BC<sub>3</sub> and graphene nanosheets.

Complexes formed by the drug molecule amantadine with nanosheets are investigated in several dimensions.

#### 4.1.1. Rimantadine complex and graphene nanosheet

The Rimantadine molecule complexes its amino moiety with the carbon atom of the graphene nanosheet through the nitrogen atom (Scheme 1). The absolute energy of this complex is about -2777103.94 kcal / mol. The absorption

energy of Ead Rimantadine and graphene nanosheet is about -2.06 kcal / mol (Table 1). The highest occupied molecular orbital (HOMO) is located at -3.74 eV and the lowest unoccupied molecular orbital (LUMO) is located at -3.56 eV. Thus, Eg is obtained at about 0.18 eV (Table 2). The Rimantadine-graphene Eg complex has not changed from the graphene nanosheet.



**Figure 1.** Optimized structure of amantadine molecule complex with graphene nanosheet.

#### 4.1.2. Amantadine complex and nanosheet BC<sub>3</sub>

The amantadine molecule can approach the BC<sub>3</sub> nanoparticle boron atom through its nitrogen atom, A complex between an N atom in Rimantadine with a free electron pair and a B atom with an empty orbital can be formed (Scheme 2). The absolute energy of this complex is about -2577537.74 kcal bermol. The adsorption energy (Ead) in the Rimantadine-BC<sub>3</sub> complex is approximately -23.96 kcal / mol (Table 1), which is higher than the Ead of the amantadine-graphene complex The highest occupied molecular orbital (HOMO) is at -6.18 and the lowest unoccupied molecular orbital (LUMO) is at -3.66 eV. Thus, Eg is obtained at about 2.51 eV (Table 2). Eg The Rimantadine-BC<sub>3</sub> complex is reduced from 2.51 to 2.71 electron volts compared to the BC<sub>3</sub> nanosheet, which is much more than the amount of the graphene-Rimantadine nanosheet.



**Figure 2.** Optimized structure of Rimantadine molecule complex with BC<sub>3</sub> nanosheet.

#### 4.1.3. Rimantadine complex and BC<sub>3</sub>-Al nanosheet

The Rimantadine molecule complexes its amino portion with the BC<sub>3</sub>-Al nanosheet aluminum atom through the nitrogen atom (Scheme 3). The absolute energy of this complex is approximately 274030.27 kcal / mol. The

adsorption energy (Ead) in the Rimantadine-nanosheet complex BC<sub>3</sub>-Al is about -28.72 kcal / mol, which is higher than the Ead of the Rimantadine-BC<sub>3</sub> complex . Table 1 presents the characteristics of the optimized

structure of the Rimantadine molecule complex with BC3-Al nanosheet. The highest occupied molecular orbital (HOMO) is at -5.66 eV and the lowest unoccupied molecular orbital (LUMO) is at -3.55 eV. Thus,  $E_g$  is obtained around eV 2.11 (Table 2).  $E_g$  The Rimantadine-BC3-Al nanosheet complex has been reduced to 2.47 electron volts compared to the BC3-Al nanosheet 2.11, which is much more than the amount of the BC3-Rimantadine nanosheet complex.

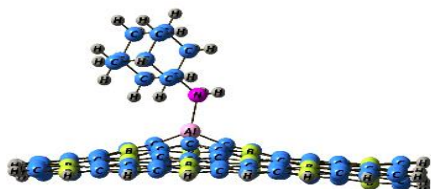


**Figure 3.** Optimized structure of Rimantadine molecule complex with BC3-Al nanosheet.

#### 4.1.4. Rimantadine complex and BC3-Si nanosheet

The Rimantadine molecule forms a complex with its BC3-Si nanosheet silicon atom through its nitrogen atom (Scheme 4). The absolute energy of this complex is approximately 2743504.36 kcal / mol. The adsorption energy ( $E_{ad}$ ) in the Rimantadine-nanosheet complex BC3-Si is about -19.32 kcal / mol, which is less than the  $E_{ad}$  of the Rimantadine-nanosheet BC3-Al complex. Table 1 presents the specifications of the optimized structure of the Rimantadine molecule complex with BC3-Si nanosheet. The highest occupied molecular orbital (HOMO) is at -4.09 eV and the lowest unoccupied molecular orbital (LUMO) is at -3.52 eV. Thus,  $E_g$  is obtained at about 0.56 eV (Table2). The Rimantadine-nanosheet complex BC3-Si is reduced from 0.56 to 1.30 electron volts compared to the BC3-Si nanosheet, which is much more than the Rimantadine-nanosheet BC3-Al complex.

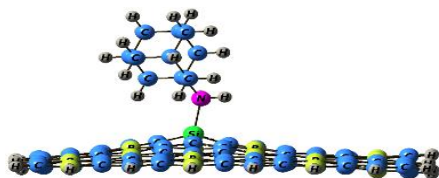
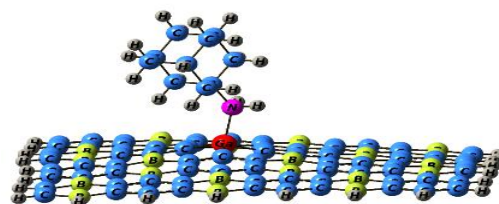


**Figure 4.** Optimized structure of Rimantadine molecule complex with BC3-Si nanosheet.

#### 4.1.5. Rimantadine complex and BC3-Ga nanosheet

The Rimantadine molecule complexes its amino moiety with the BC3-Ga nanosheet gallium atom through its nitrogen atom (Scheme 5). The absolute energy of this

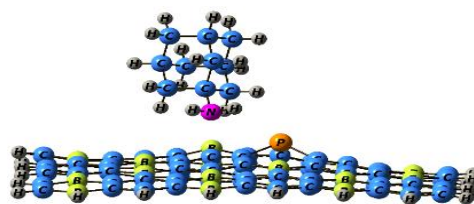
complex is approximately 3768489.43 kcal / mol. The adsorption energy ( $E_{ad}$ ) in the Rimantadine-nanosheet complex BC3-Ga is approximately -20.41 kcal / mol, which is higher than the  $E_{ad}$  of the Rimantadine-nanosheet complex BC3-Si. Table 1 presents the characteristics of the optimized structure of the Rimantadine molecule complex with BC3-Ga nanosheet. The highest occupied molecular orbital (HOMO) is -5.85 at eV and the lowest unoccupied molecular orbital (LUMO) is -3.66 at eV. Thus,  $E_g$  is obtained at about 2.19 eV (Table2). The Rimantadine-nanosheet complex of BC3-Ga is reduced from 2.19 to 2.41 electron volts compared to the BC3-Ga nanosheet, which is less than the amount of Rimantadine-nanosheet BC3-Si complex.



**Figure 5.** Optimized structure of Rimantadine molecule complex with BC3-Ga nanosheet.

#### 4.1.7. Rimantadine complex and BC3-P nanosheet

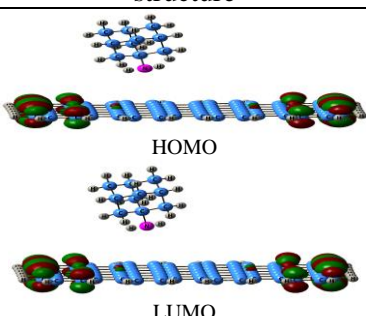
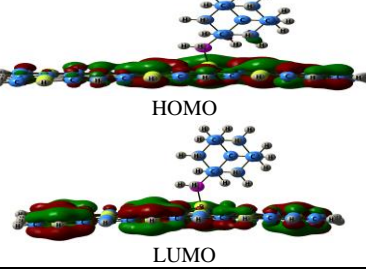
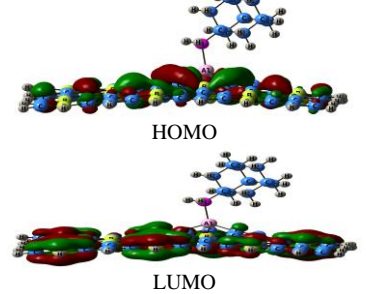
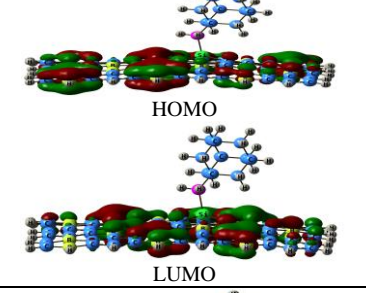
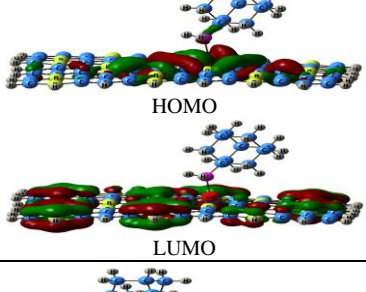
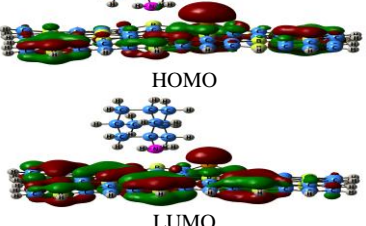
The Rimantadine molecule forms a complex with the BC3-P nanosheet phosphorus atom through its nitrogen atom (Scheme 6). The absolute energy of this complex is approximately 277612018.03 kcal / mol. The adsorption energy of  $E_{ad}$  in the Rimantadine-nanosheet complex BC3-P is about -20.31 kcal / mol, which is less than the  $E_{ad}$  of the Rimantadine-nanosheet BC3-Ga complex. Table 1 presents the characteristics of the optimized structure of the Rimantadine molecule complex with BC3-P nanosheet. The highest occupied molecular orbital (HOMO) is at -5.83 eV and the lowest unoccupied molecular orbital (LUMO) is at -3.55 eV. Thus,  $E_g$  is obtained at about 2.28 eV (Table2). The Rimantadine-nanosheet complex BC3-P has increased from 2.28 to 2.17 electron volts compared to the Rimantadine nanosheet complex BC3-P, which is not appropriate at all.



**Figure 6.** Optimized structure of Rimantadine molecule complex with BC3-P nanosheet.



**Table 3.** Rimantadine drug molecule complexes with BC<sub>3</sub> nanoplate and BC<sub>3</sub> doped in terms of Homo-Lomo energy

name	structure
Rimantadine-Graphene	 <p>HOMO</p> <p>LUMO</p>
Rimantadine-BC <sub>3</sub>	 <p>HOMO</p> <p>LUMO</p>
Rimantadine-BC <sub>3</sub> -Al	 <p>HOMO</p> <p>LUMO</p>
Rimantadine-BC <sub>3</sub> -Si	 <p>HOMO</p> <p>LUMO</p>
Rimantadine-BC <sub>3</sub> -Ga	 <p>HOMO</p> <p>LUMO</p>
Rimantadine-BC <sub>3</sub> -P	 <p>HOMO</p> <p>LUMO</p>

## 5. Conclusion

In conclusion The interactions between the Rimantadine molecule and nanoparticles including graphene, BC<sub>3</sub>, and doped BC<sub>3</sub> with aluminum, silicon, phosphorus and gallium atoms have been studied using the B3LYP method with a basis set of 6-31G(d) by Gaussian software 09. The interaction between the Rimantadine drug molecule and the graphene nanoparticle show a poor energy interactions to Rimantadine. The interaction between the BC<sub>3</sub> nanosheet and the amantadine drug was also studied. The E<sub>ad</sub> (adsorption energy) and E<sub>g</sub> (gap energy) of BC<sub>3</sub> and doped nanosheet particles to Rimantadine were studied.

- ✓ The changes in E<sub>ad</sub> for complexes are as follows:  

$$\text{BC}_3\text{-Al/Rimantadine} > \text{BC}_3\text{/Rimantadine} > \text{BC}_3\text{-Ga/Rimantadine} > \text{BC}_3\text{-P/Rimantadine} > \text{BC}_3\text{-Si/Rimantadine} > \text{Graphene/Rimantadine}$$
  - ✓ The changes in E<sub>g</sub> for complexes are as follows:  

$$\text{BC}_3\text{-Si/Rimantadine} > \text{BC}_3\text{-Al/Rimantadine} > \text{BC}_3\text{-Ga/Rimantadine} > \text{BC}_3\text{/Rimantadine} > \text{Graphene/Rimantadine} > \text{BC}_3\text{-P/Rimantadine}$$
- We conclude that the doped BC<sub>3</sub> nanoparticle with silicon atom is the best sensor for Rimantadine drug.

## Acknowledgements

We are grateful for the support of Shahid Madani University of Tabriz, Tabriz University and also Payame Noor University, Tabriz Branch.

## References

- [1] A. Haghighi Asl, A. Ahmadpour, N. Fallah, Synthesis of Nano N-TiO<sub>2</sub> for modeling of petrochemical industries spent caustic wastewater photocatalytic treatment in visible light using DOE method, *Applied Chemistry*, 12 (2017) 253-286.
- [2] A. Ahmadpour, AH. Asl, N. Fallah, Synthesis and comparison of spent caustic wastewater photocatalytic treatment efficiency with zinc oxide composite, *Desalination and Water Treatment*, 92 (2017) 275-290.
- [3] M. J. Allen, V. C Tung, R. B.Kaner, Honeycomb carbon: a review of graphene. *Chemical reviews*. 110 (2009) 132-145.
- [4] D. R. Dreyer, R. S. Ruoff, From conception to realization: an historial account of graphene and some perspectives for its future. *Angewandte Chemie International Edition*., (2010) 49 (49), 9336-9344.
- [5] S. Park, R. S. Ruoff, Chemical methods for the production of graphenes. *Nature nanotechnology*., (2009) 4 (4), 217.
- [6] Y. Zhu, S. Murali, W. Cai, , Potts, J. R.; Ruoff, R. S., Graphene and graphene oxide: synthesis, properties, and applications. *Advanced materials* 2010, 22 (35), 3906-3924.
- [7] J. Mashhadizadeh, A. Bozorgian, A. Azimi, Investigation of the kinetics of formation of Clatrit-like dual hydrates TBAC in the presence of CTAB, *Eurasian Chemical Communication*, 2 (2020), 536-547.

- [8] M. Bagheri Sadr, A. Bozorgian, An Overview of Gas Overflow in Gaseous Hydrates, *Journal of Chemical Reviews*, 3 (2021), 66-82.
- [9] Y. Ding, Y. Wang, J. Ni, Structural, electronic, and magnetic properties of defects in the BC3 sheet from first principles. *The Journal of Physical Chemistry C*, (2010) 114 (29) 12416-12421.
- [10] A. Bozorgian, B. Raei, Thermodynamic modeling and phase prediction for binary system dinitrogen monoxide and propane, *Journal of Chemistry Letters*, 1 (2020), 143-148.
- [11] I. A. Popov, A. I. Boldyrev, Deciphering chemical bonding in a BC3 honeycomb epitaxial sheet. *The Journal of Physical Chemistry C*, (2012) 116 (4) 3147-3152.
- [12] F. Chuang, Z. Huang, W. Lin, Albao, M. A.; Su, W.-S., Structural and electronic properties of hydrogen adsorptions on BC3 sheet and graphene: a comparative study. *Nanotechnology* (2011) 22 (13) 135703.
- [13] D. C. Young, A Practical Guide for Applying Techniques to Real-World Problems. Wiley–Interscience New York: (2001).
- [14] E. G. Lewars, *Computational chemistry: introduction to the theory and applications of molecular and quantum mechanics*. Springer Science & Business Media: (2010).
- [15] T. van Mourik, M. Bühl, M.; Gageot, Density functional theory across chemistry, physics and biology. The Royal Society: (2014).
- [16] A. Bozorgian, Investigation of the effect of Zinc Oxide Nano-particles and Cationic Surfactants on Carbon Dioxide Storage capacity, *Advanced Journal of Chemistry, Section B: Natural Products and Medical Chemistry*, 3 (2021) 54-61.
- [17] M. Austin-Seymour, I. Kalet, J. McDonald, Three dimensional planning target volumes: a model and a software tool. *International Journal of Radiation Oncology\* Biology\* Physics*, (1995) 33 (5), 1073-1080.
- [18] Landa, S.; Macháček, V., Sur l'adamantane, nouvel hydrocarbure extrait du naphte. *Collection of Czechoslovak Chemical Communications* (1933) 5, 1-5.
- [19] M. M. Kadhim, E. A. Mahmood, V. Abbasi, M. R. Poor Heravi, S. Habibzadeh, S. Mohammadi-Aghdam, S. M. Shoaie, Theoretical investigation of the titanium—nitrogen heterofullerenes evolved from the smallest fullerene, *J. Mol. Graph. Model.* 117 (2022) 108269.
- [20] S.M. Hosseini, H. Hosseini-Monfared, V. Abbasi, Silver ferrite–graphene nanocomposite and its good photocatalytic performance in air and visible light for organic dye removal, *Applied Organometallic Chemistry* 31 (2017) e3589.
- [21] V. Abbasi, H. Hosseini-Monfared, S. M. Hosseini, Mn (III)-salan/graphene oxide/magnetite nanocomposite as a highly selective catalyst for aerobic epoxidation of olefins, *Applied Organometallic Chemistry*, 31 (2017) e3554.
- [22] V. Abbasi, H. Hosseini-Monfared, S. M. Hosseini, A heterogenized chiral imino indanol complex of manganese as an efficient catalyst for aerobic epoxidation of olefins, *New Journal of Chemistry*, 41 (2017) 9866-9874.
- [23] M. Hosseini, H. Hosseini-Monfared, V. Abbasi, M. R. Khoshroo, Selective oxidation of hydrocarbons under air using recoverable silver ferrite–graphene (AgFeO<sub>2</sub>–G) nanocomposite: A good catalyst for green chemistry, *Inorg. Chem. Comm.* 67 (2016) 72-79.
- [24] H. Hosseini Monfared, V. Abbasi, A. Rezaei, M. Ghorbanloo, A. Aghaei, A heterogenized vanadium oxo-aroilydrazone catalyst for efficient and selective oxidation of hydrocarbons with hydrogen peroxide, *Transition Metal Chemistry*, 37 (2012) 85-92.